

Photochemical Properties of Formaldehyde

Nicolás Rojo Esteban



1 Introduction

Formaldehyde (H_2CO) is the simplest and most common of the carbonyl compounds, it has an important role in atmospheric chemistry, interstellar media, and combustion processes. In the troposphere, it is an intermediate in the oxidation of many volatile organic compounds and a major source of hydroperoxyl radicals (HO_2), These HO_2 radicals react with NO to form OH and NO_2 , giving rise to the $\text{NO}_x \rightarrow \text{O}_3$ reaction and therefore regulating ozone levels and air quality [1]. In the interstellar medium, specifically in molecular clouds, formaldehyde adsorbed onto icy dust grains can undergo UV-driven reactions that lead to the formation of more complex organic molecules, therefore the photochemistry of formaldehyde is also very important in astrochemical modeling [2].

The photochemistry of formaldehyde has two principal electronic transitions: a weak $n \rightarrow \pi^*$ band in the near-UV (300nm, 4.1eV) and a much stronger $\pi \rightarrow \pi^*$ band in the UV (185nm, 6.7eV) [3, 4, 5]. Photoexcitation into these states leads to non-radiative dissociation into $\text{CO} + \text{H}_2$ and other radical fragments, with a fluorescence probability below 10^{-4} [4].

In this work, I will focus on the calculation of the vertical excitation energies and oscillator strengths of the $n \rightarrow \pi^*$ and $\pi \rightarrow \pi^*$ transitions, and I will use CASSCF and RMS-CASPT2 optimized geometries.

2 Computational Details

All electronic structure calculations were performed with the OpenMolcas program[6], using a complete active space self-consistent field (CASSCF)[7] with an active space of six electrons in four orbitals (CAS(6,4)). Dynamic correlation was then treated using the relaxed multistate CASPT2 (RMS-CASPT2)[8]. Finally, transition dipole moments and oscillator strengths were computed via the RASSI module[9].

The discrete oscillator strengths were processed into continuous spectra by broadening the bands with a Gaussian function of Full Width at Half Maximum of 0.30 eV (FWHM = 0.30 eV) using Python (v3.8), and Matplotlib[10].

3 Results

3.1 Discussion of the choice of active space

In order to accurately describe the electronic states of formaldehyde ($\text{H}_2\text{C=O}$) using multiconfigurational methods such as CASSCF, it is essential to choose an appropriate active space. The active space should include the orbitals that play a key role in the electronic excitations and chemical reactivity of the molecule.

For formaldehyde, the most relevant orbitals are:

1. **The nonbonding orbital on oxygen (n_O):** This orbital is localized on the oxygen atom and it is very important for describing the $n \rightarrow \pi^*$ excitation.

2. **The π bonding orbital:** This orbital represents the electron density shared between the carbon and oxygen atoms in the carbonyl group and is important for the ground-state electronic structure.
3. **The π^* antibonding orbital:** This orbital is involved in the electronic excitations, particularly in the $n \rightarrow \pi^*$ and $\pi \rightarrow \pi^*$ transitions.

So, at first I decided to use a CAS(4,3) active space including these three orbitals and the four electrons in the bonding ones. However, later I had to include an extra orbital, leading to an extension of the active space to CAS(6,4). The reason for this enlargement of the active space will be discussed afterwards.

Starting from the chosen CAS reference, I performed a self-consistent field (SCF) calculation followed by a CASSCF calculation to obtain the one and two-electron integrals, and an initial set of molecular orbitals.

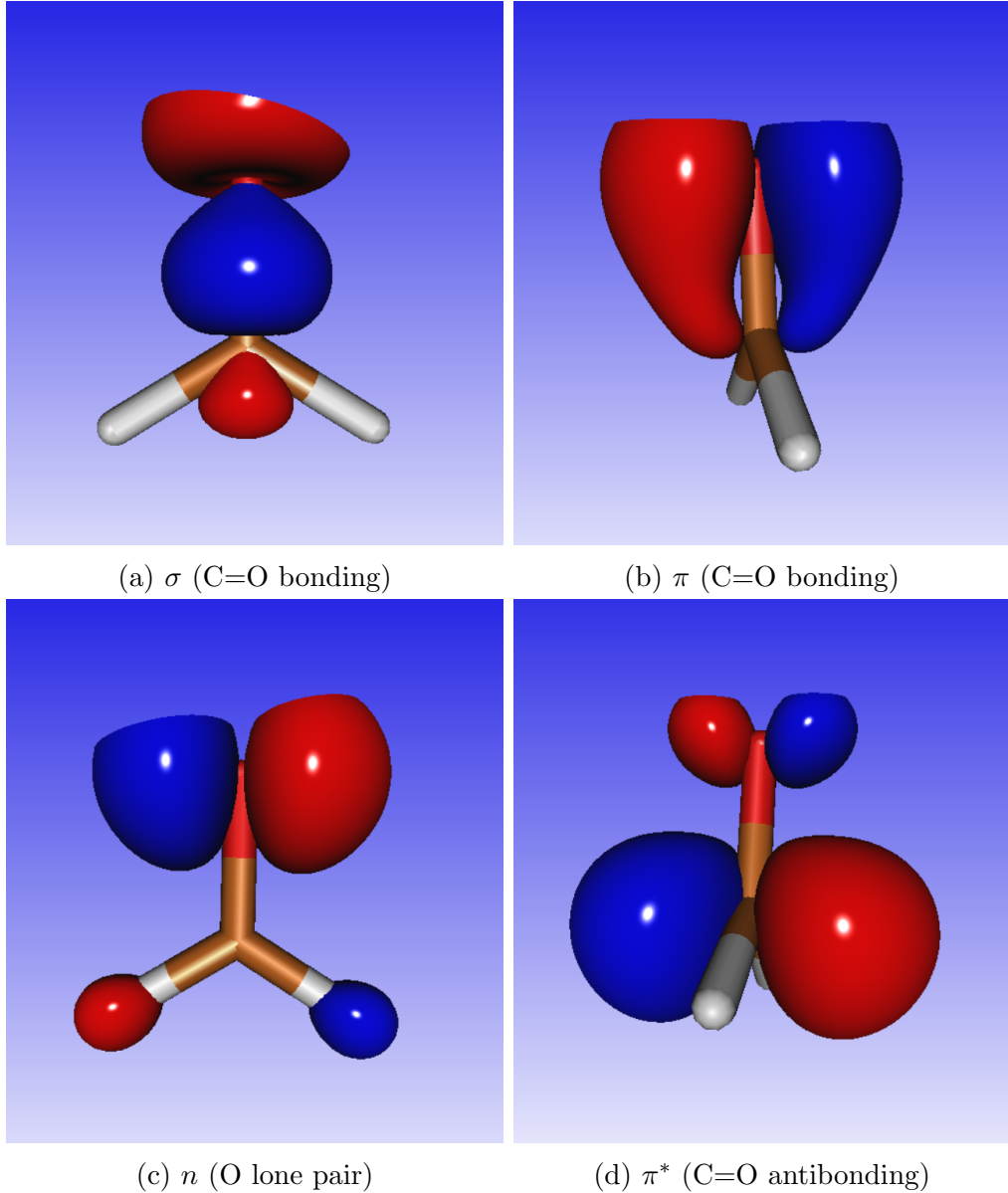


Figure 1: Active molecular orbitals used in the CAS(6,4) reference, rendered at an isovalue of 0.1 au.

3.2 Ground-State Geometry Optimization

The next step involved optimizing the ground-state geometry at the CASSCF level. Although the original protocol called for a state-specific CASSCF on the single lowest root, I accidentally ended up using a state-averaged CASSCF over four roots. Here I noticed that the initial active space of CAS(4,3) was not enough since the program automatically included the $\sigma(\text{C}=\text{O})$ bonding orbital in the active space and, in doing so, excluded the $\pi(\text{C}=\text{O})$ bonding orbital that is critical for describing the $\pi \rightarrow \pi^*$ excitations. This reflects that the $\sigma(\text{C}=\text{O})$ orbital likely plays a significant role in the ground-state potential energy surface. To fix this and ensure the $\pi(\text{C}=\text{O})$ orbital remained active, I changed the active

space to CAS(6,4).

3.3 Vertical Excitation Energies and Oscillator Strengths of the Ground State

Vertical excitation energies were calculated using the RMS-CASPT2 method with a state-averaged reference over four roots and the active space of CAS(6,4). The RMS (relaxed multistate) variant of CASPT2 refines the multistate CASPT2 method by using state-specific correlation-relaxed Fock operators.

Following the RMS-CASPT2 calculation, I used the RASSI module to evaluate transition dipole moments and derive oscillator strengths for each vertical excitation. By doing this two steps I obtained both the excitation energies ΔE_i and oscillator strengths f_i .

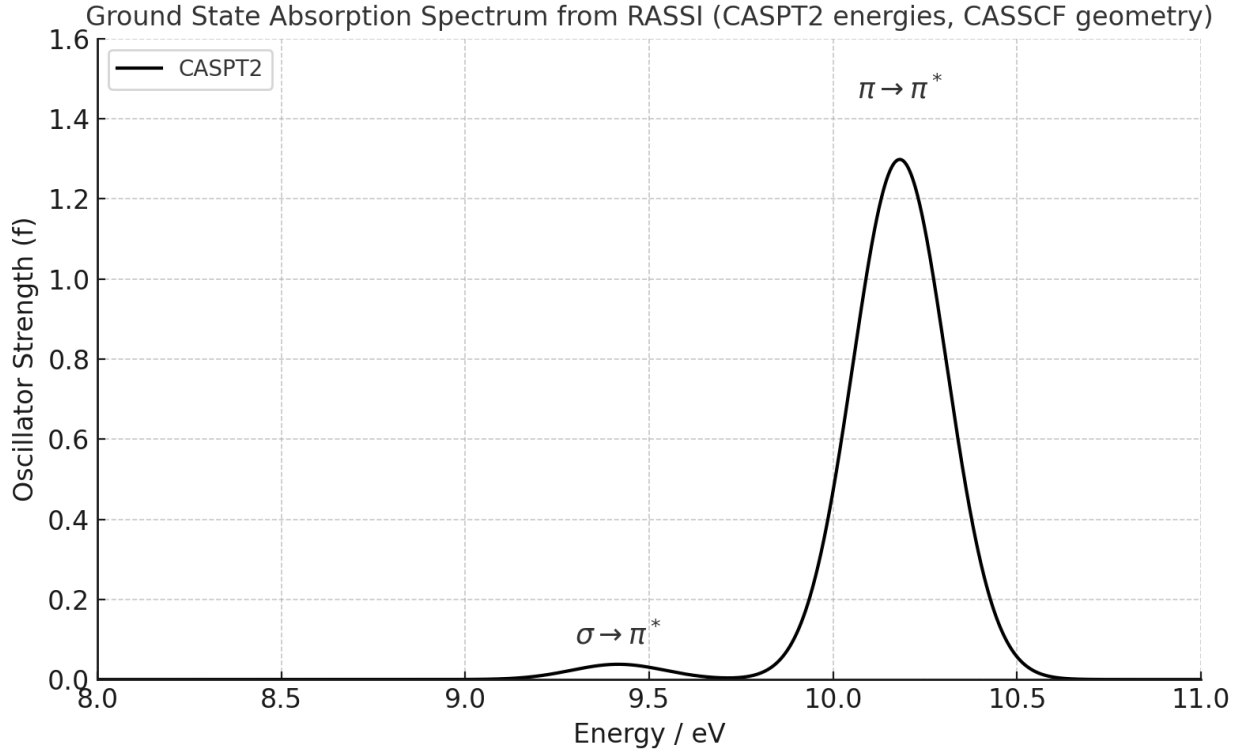


Figure 2: Ground-state absorption spectrum of the formaldehyde at the **RMS-CASPT2//CASSCF** level. FWHM = 0.30 eV Gaussian broadening

Table 1: Vertical excitation energies for the $\sigma \rightarrow \pi^*$ and $\pi \rightarrow \pi^*$ transitions at the **RMS-CASPT2//CASSCF** level compared to gas-phase experiment.

Transition	Theory (eV)	Oscillator Strength (f)	Experiment (eV)
$\sigma \rightarrow \pi^*$	9.4159	1.2140×10^{-2}	9.00 [11]
$\pi \rightarrow \pi^*$	10.1816	4.1459×10^{-1}	6.70 [4]

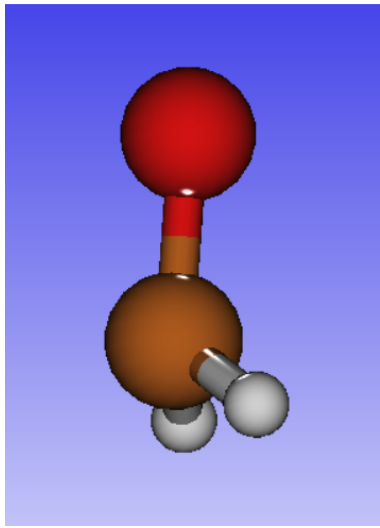
Figure 2 reveals the following:

- **$\sigma \rightarrow \pi^*$ band (~ 9.42 eV):** Exhibits a low oscillator strength ($f \approx 10^{-2}$). By the electric-dipole selection rules, its transition dipole moment is small because the overlap between the $\sigma(\text{C}=\text{O})$ bonding orbital and the $\pi^*(\text{C}=\text{O})$ antibonding orbital is minimal.
- **$\pi \rightarrow \pi^*$ band (~ 10.18 eV):** Shows a much higher intensity ($f \approx 4 \times 10^{-1}$), consistent with a larger dipole moment arising from good spatial overlap between the $\pi(\text{C}=\text{O})$ and $\pi^*(\text{C}=\text{O})$ orbitals.
- **$n \rightarrow \pi^*$ band:** Not observable in the spectrum with $f < 10^{-10}$, since the oxygen lone-pair (n) orbital has negligible overlap with the π^* orbital and therefore a very small transition dipole.

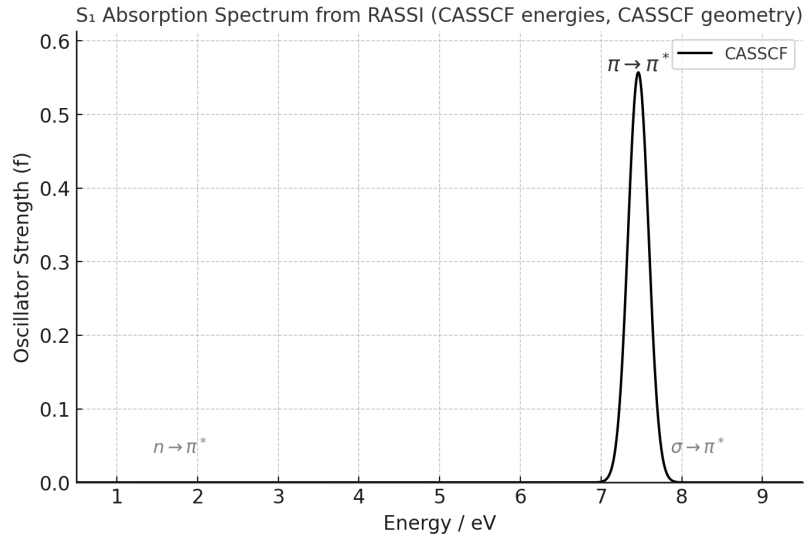
In terms of energy, the computed peak at ~ 10.18 eV contrast with the gas-phase experimental value of 6.70 eV for the $\pi \rightarrow \pi^*$ maximum.[4, 3] This ~ 3.5 eV blue shift can be attributed to the 6-31G* basis set, since it is a relatively small basis, specially for a four-atom molecule, even when using RMS-CASPT2 to account for dynamic correlation. With respect to the ~ 9.42 eV value for the $\sigma \rightarrow \pi^*$ peak it is relatively similar to the experimental value of 9.00eV [11].

3.4 First Excited-State (S_1) Geometry and Spectrum

After optimizing the S_1 geometry at the CASSCF(6,4) level (state-averaged over four roots), I found that formaldehyde distorts from the planar ground state into a pyramidal geometry (Figure 3a). After, I did a harmonic frequency analysis (Hessian) whcih confirmed that there were no imaginary modes, proving this as a true minimum. Finally, vertical oscillator strengths were computed with RASSI on the CASSCF(6,4) reference to produce the absorption spectrum shown in Figure 3b.



(a) CASSCF(6,4) S_1 geometry



(b) S_1 absorption spectrum (CASSCF energies, CASSCF geometry, FWHM = 0.30eV)

Figure 3: (a) Pyramidal S_1 structure. (b) Gaussian-broadened spectrum showing only the $\pi \rightarrow \pi^*$ band at $\sim 7.46\text{eV}$.

Table 2: Vertical excitation energies and oscillator strengths from the S_1 minimum (CASSCF(6,4) geometry) at the CASSCF level.

Transition	Energy (eV)	Oscillator Strength (f)
$n \rightarrow \pi^*$	1.7810	6.07×10^{-4}
$\pi \rightarrow \pi^*$	7.4616	1.78×10^{-1}
$\sigma \rightarrow \pi^*$	8.1978	5.84×10^{-4}

For a molecule to show fluorescence, two conditions must be met:

1. Dipole-allowed emissive transition: The excited state must have a nonzero oscillator strength ($f > 0$) for the radiative $S_1 \rightarrow S_0$ transition.
2. Radiative rate: The spontaneous emission rate $k_{\text{fl}} \propto f \Delta E^2$ must be higher than all nonradiative decay rates (k_{nr}).

In formaldehyde:

- The S_1 state is of $n \rightarrow \pi^*$ character, with $f \approx 0$. Therefore k_{fl} is essentially zero.
- Nonradiative decay (internal conversion through an S_1/S_0 conical intersection and intersystem crossing) depletes the S_1 population faster than any fluorescence can occur.

Therefore, although the oscillator strength is not zero and S_1 can be populated by absorption, it cannot emit via fluorescence.

3.5 RMS-CASPT2 Geometry Optimizations and Absorption Spectra of S_0 and S_1

Both the ground state (S_0) and the first excited state (S_1) were fully optimized at the RMS-CASPT2 level (CAS(6,4), state-averaged over four roots). Vertical excitation energies and oscillator strengths were then obtained with the RASSI module using CASPT2 energies on these CASPT2 geometries.

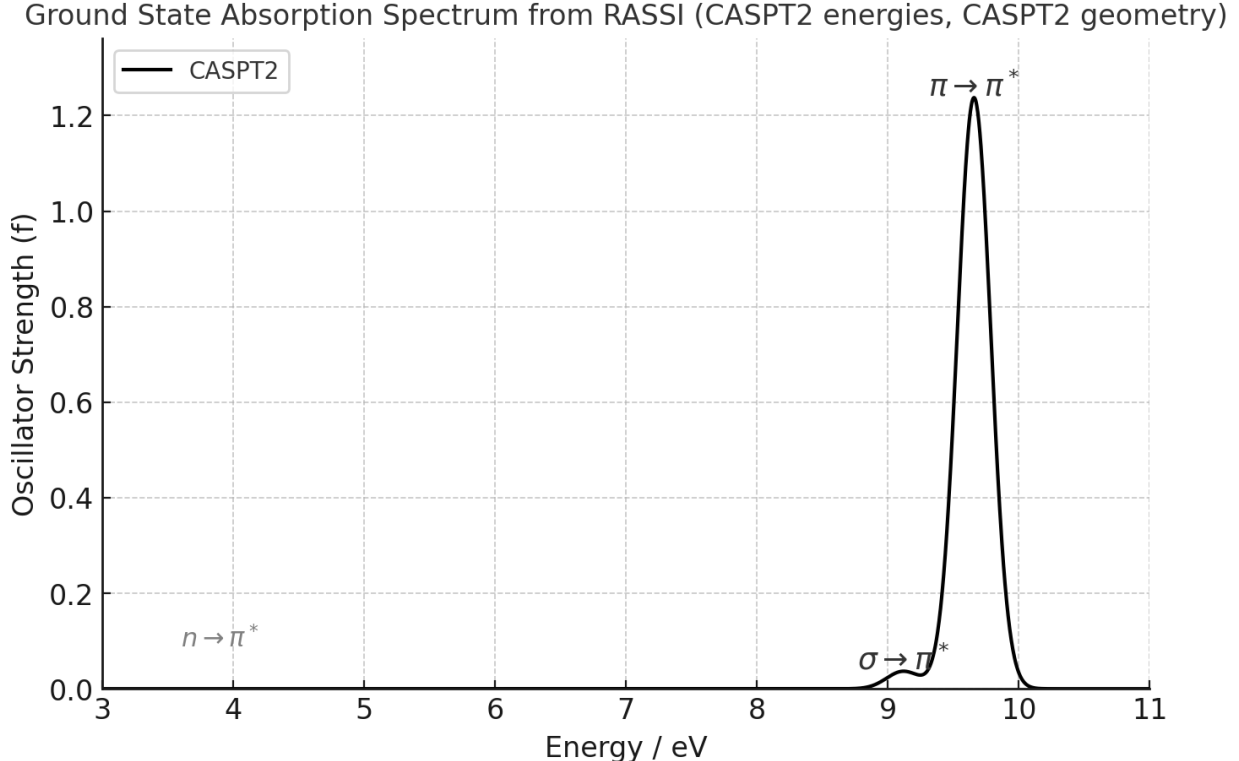


Figure 4: Ground state absorption spectrum (RASSI/CASPT2 energies on CASPT2 geometry).

Table 3: Transitions on the CASPT2-optimized ground-state geometry.

Transition	Energy (eV)	Oscillator Strength (f)
$n \rightarrow \pi^*$	3.9006	3.19×10^{-10}
$\sigma \rightarrow \pi^*$	9.1183	1.17×10^{-2}
$\pi \rightarrow \pi^*$	9.6587	3.95×10^{-1}

Using the CASSCF(6,4) optimized geometry and RASSI/CASPT2 energies, the vertical bands appear at:

$$\sigma \rightarrow \pi^* : 9.42 \text{ eV}, \quad \pi \rightarrow \pi^* : 10.18 \text{ eV}.$$

With the re-optimized the S_0 geometry at the RMS-CASPT2 level the new bands appear at:

$$\sigma \rightarrow \pi^* : 9.12 \text{ eV}, \quad \pi \rightarrow \pi^* : 9.66 \text{ eV},$$

bringing the $\sigma \rightarrow \pi^*$ band closer to the experimental value of 9.00eV, while the $\pi \rightarrow \pi^*$ transition remains overestimated (experimental ≈ 6.70 eV). This demonstrates that inclusion of dynamic correlation in the geometry optimization improves accuracy, although the small 6-31G* basis is still not enough for a good quantitative prediction of the $\pi \rightarrow \pi^*$ energy.

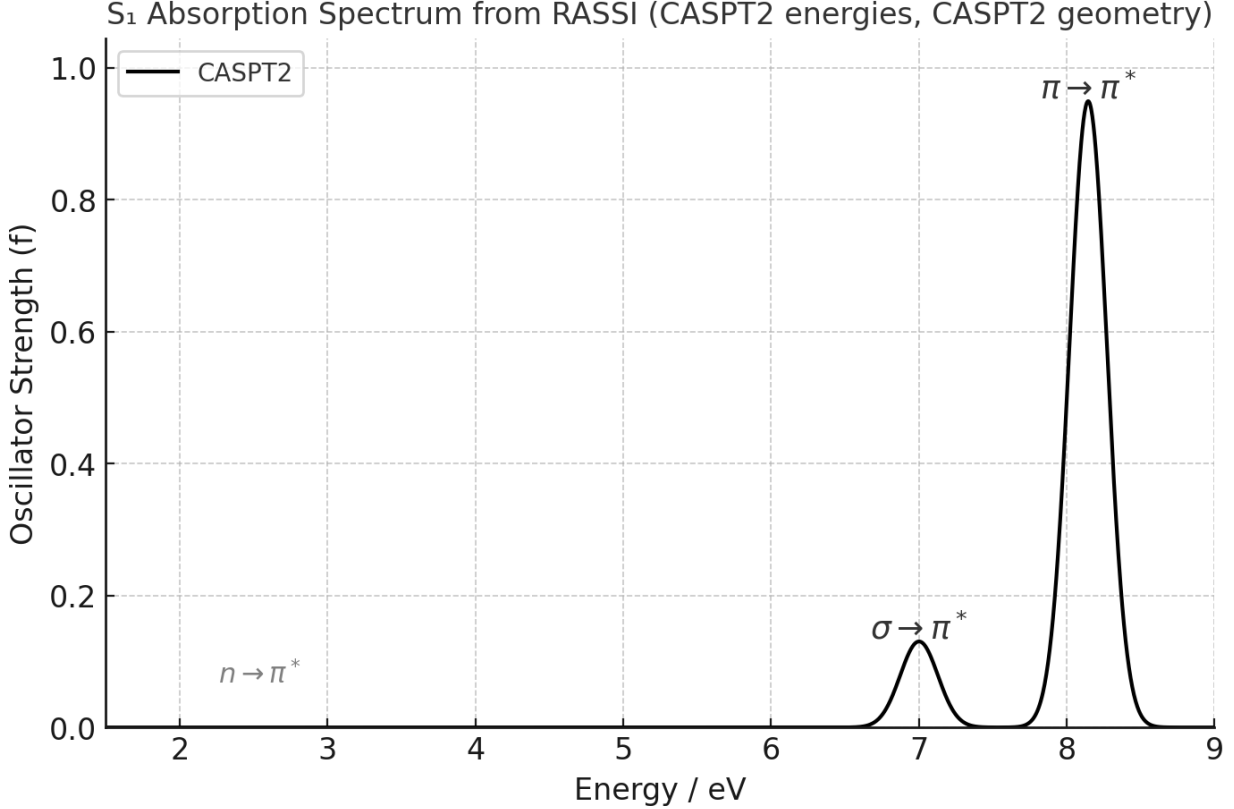


Figure 5: S_1 absorption spectrum (RASSI/CASPT2 energies on CASPT2 geometry).

Table 4: Transitions on the CASPT2-optimized first excited-state geometry.

Transition	Energy (eV)	Oscillator Strength (f)
$n \rightarrow \pi^*$	2.5395	2.66×10^{-4}
$\sigma \rightarrow \pi^*$	7.0021	4.16×10^{-2}
$\pi \rightarrow \pi^*$	8.1464	3.03×10^{-1}

At CASSCF(6,4) level with using CASSCF-optimized geometries and RASSI/CASSCF energies, the vertical bands from S_1 occur at

$$\pi \rightarrow \pi^* : 1.78 \text{ eV}, \quad \pi \rightarrow \pi^* : 7.46 \text{ eV}, \quad \sigma \rightarrow \pi^* : 8.20 \text{ eV}.$$

When both the S₁ geometry and vertical energies are calculated at RMS-CASPT2, these shift to:

$$n \rightarrow \pi^* : 2.54 \text{ eV}, \quad \sigma \rightarrow \pi^* : 7.00 \text{ eV}, \quad \pi \rightarrow \pi^* : 8.15 \text{ eV}.$$

When using the CASSCF level the tendency was $E(\pi \rightarrow \pi^*) \approx 7.46 \text{ eV} < E(\sigma \rightarrow \pi^*) \approx 8.20 \text{ eV}$ which does not match with the molecular orbitals, since the occupied π MO is lower in energy than the σ MO. When dynamic correlation is added via RMS-CASPT2 (both geometry and energies), the order is switched into $E(\sigma \rightarrow \pi^*) \approx 7.00 \text{ eV} < E(\pi \rightarrow \pi^*) \approx 8.15 \text{ eV}$. Although there are no experimental vertical energies available for S₁ since it is an excited state, this qualitative correction strongly suggests that including dynamic correlation can improve the predictions of excited state energies in this molecule.

4 Conclusions

In this work I have studied the photochemistry of formaldehyde in both its ground (S₀) and first excited state (S₁) using a CAS(6,4) active space that includes the oxygen lone pair (n), the $\pi(\text{C}=\text{O})$ bonding orbital, and the $\pi^*(\text{C}=\text{O})$ antibonding. Absorption spectra were first computed on CASSCF-optimized geometries and then on RMS-CASPT2-optimized geometries. Qualitatively, the computed oscillator strengths for the $n \rightarrow \pi^*$ and $\sigma \rightarrow \pi^*$ bands are essentially zero, while the $\pi \rightarrow \pi^*$ band is intense, this result is consistent with the selection rules and it means that there is a high probability of excitation into the $\pi \rightarrow \pi^*$ (root 4) state. Quantitatively, the vertical energies of these bands on the ground-state geometry (9.42 and 10.18eV at CASSCF; 9.12 and 9.66eV at CASPT2) are significantly blue-shifted in comparison to the experimental values (9.00 and 6.70eV), this discrepancy can be attributed to the small 6-31G* basis set. Although inclusion of dynamic correlation in the geometry optimization (RMS-CASPT2) improves the predicted energies by up to 0.3–0.5eV, the results still are far from experiment.

References

- [1] R. Cantrell and G. K. Moortgat, J. Phys. Chem. **94** (1990) 3902–3910.
- [2] S. B. Sunanda, R. E. Showalter, I. Kanik, and R. J. Emrich, Spectrosc. Lett. **45** (2012) 65–72.
- [3] J. E. Mentall, E. P. Gentieu, and M. Krauss, J. Chem. Phys. **55** (1971) 5471–5478.
- [4] M. Suto, X. Wang, and L. C. Lee, J. Chem. Phys. **85** (1986) 4228–4233.
- [5] D. J. Pope *et al.*, Faraday Discuss. **130** (2005) 59–72.
- [6] L. González, D. Astruc, F. Fdez. Galván *et al.*, J. Chem. Theory Comput. **15** (2019) 5925–5964.
- [7] B. O. Roos, P. R. Taylor, and P. E. M. Sigbahn, Chem. Phys. **48** (1980) 157–173.
- [8] K. Andersson, P.-Å. Malmqvist, and B. O. Roos, J. Chem. Phys. **96** (1992) 1218–1226.

- [9] F. Aquilante *et al.*, J. Comput. Chem. **31** (2010) 224–247.
- [10] J. D. Hunter, Comput. Sci. Eng. **9** (2007) 90–95.
- [11] R. Meller and G. K. Moortgat, J. Geophys. Res. **105** (2000) 7089–7101.